

Experimental disentangling of orbital and lattice energy scales by inducing cooperative Jahn-Teller melting in $\text{KCu}_{1-x}\text{Mg}_x\text{F}_3$ solid solutions

Paolo Ghigna,^{1,*} Marco Scavini,² Claudio Mazzoli,³ Michela Brunelli,⁴ Claudio Laurenti,¹ and Claudio Ferrero³

¹*IENI-CNR and Dipartimento di Chimica Fisica, Università di Pavia, Viale Taramelli 16, I-27100 Pavia, Italy*

²*Dipartimento di Chimica Fisica ed Elettrochimica, Università di Milano, V. Golgi 19, I-20133 Milano, Italy*

³*European Synchrotron Radiation Facility, 6, av. J. Horowitz, BP 220, 38043 Grenoble Cedex, France*

⁴*Institut Laue Langevin, 6, av. J. Horowitz, BP 156, 38042 Grenoble Cedex 9, France*

(Received 28 January 2010; published 23 February 2010)

The melting of the cooperative Jahn-Teller distortion (cJTd) in $\text{KCu}_{1-x}\text{Mg}_x\text{F}_3$ has been studied by high-resolution x-ray powder diffraction. A first-order phase transition relaxing the cJTd is detected at temperatures increasing monotonically with x . From the transition temperatures, an estimate of the cJTd stabilization energy is derived and found to be linearly increasing with x . By extrapolating to $x=0$, the cJTd energy in the parent compound KCuF_3 is determined. It is argued how, in the light of current theories, the cJTd rather than orbital polarization controls the peculiar physics of KCuF_3 .

DOI: [10.1103/PhysRevB.81.073107](https://doi.org/10.1103/PhysRevB.81.073107)

PACS number(s): 71.70.Ej, 61.05.cp, 64.70.K-, 81.30.-t

I. INTRODUCTION

Strongly correlated electron systems are one of the main focuses of current research in solid state physics and advanced material science. Such systems offer both theoretical challenges and possibly exploitable opportunities for new advanced devices, as it is the case for colossal magnetoresistive materials. As several degrees of freedom can be intimately interconnected, the identification of the leading interaction and real order parameter in a phase transition often results in a very challenging task. In this context, a typical example is the interplay between the orbital ordering (OO) and the cooperative Jahn-Teller distortion (cJTd). In a seminal work, Kugel and Khomskii¹ showed how, in presence of strong electron correlation, orbitals are subject to superexchange interaction. In this case a pre-existing orbital degeneracy tends to amplify any lattice instability resulting in OO driving cJTd. In this scenario, the pseudocubic perovskite KCuF_3 has always been considered as a model system for testing the Kugel-Khomskii model. Indeed its peculiar low-dimensional magnetic behavior realized on a pseudocubic lattice can be understood only if OO is taken into consideration.² However, very recent LDA+DMFT calculations by Pavarini *et al.*³ showed that the superexchange mechanisms in KCuF_3 is not strong enough to stabilize the OO experimentally observed up to $T=800$ K.⁴ According to the calculations in Ref. 3, at this temperature the superexchange mechanisms and the electron-phonon coupling are of comparable magnitude, leaving open the question on how structural (cJTd) and orbital (OO) degrees of freedom interact. To understand this intriguing situation a deeper experimental investigation is required. Since the work of Binggeli and Altarelli,⁵ it is well known that resonant x-ray scattering (RXS) at Cu K edge cannot directly access the OO. Indeed the signal in KCuF_3 is dominated by the distortion in the coordination polyhedron of Cu, the Cu $3d$ ordering giving only a small contribution. On the other hand, the investigation of the cJTd relaxation of KCuF_3 is hard to be carried out, owing to its decomposition at T slightly higher than ~ 800 K.

In a recent paper by our group, the first experimental evidence of temperature induced melting of cJTd in a KCuF_3

related system ($\text{KCu}_{0.8}\text{Mg}_{0.2}\text{F}_3$) was reported,⁶ and $kT=0.05$ eV was obtained as a coarse estimation of the stabilization energy of the cJT-distorted phase compared to the cubic one for the above composition. In this work we present the structural phase diagram for the $\text{KCu}_{1-x}\text{Mg}_x\text{F}_3$ series, allowing for an estimate of cJTd stabilization energy for the whole series of investigated compounds, including lower Mg concentrations. In particular, the extrapolation to $x=0$ of experimental results gives the unprecedented opportunity to extract the energy scale of cJTd in the prototype compound KCuF_3 . Data presented below, hence, allow disentangling the different energy scales relevant to the physics of pure KCuF_3 . In particular, our results are shown to be in pretty good agreement with calculations performed by Pavarini *et al.*,³ strongly supporting the conclusion that cJTd (and not OO) rules the high-temperature physics of KCuF_3 . We believe that such an approach could be fruitfully generalized to other strongly correlated electron systems.

II. EXPERIMENT

$\text{KCu}_{1-x}\text{Mg}_x\text{F}_3$ samples with the tetragonal structure at room temperature (RT), i.e., with $0.1 \leq x \leq 0.25$,⁷ were synthesized by solid state reactions, starting from appropriate amounts of KCuF_3 and KMgF_3 . These materials were powdered and carefully mixed in a *Siemens mBRAUN UNIlab* dry box able to keep $p(\text{O}_2) < 1$ ppm and $p(\text{H}_2\text{O}) < 1$ ppm. The samples obtained ($x=0.10, 0.13, 0.15, 0.20, 0.25$) were pelletized in a Pt crucible put in a quartz vial. The pellets were surrounded by sheets of metallic Zr to capture the oxygen in the reaction chamber. They were kept in flowing argon (2 l/h) at 1020 K for approximately 1 h and eventually quenched to RT. KCuF_3 was prepared by a solution route according to Ref. 8. KMgF_3 was prepared by solid state reaction of KF (Aldrich, 99%) and MgF_2 (Unaxis Materials, 99.99%).

The (polycrystalline) samples were loaded and sealed in 0.8-mm-diameter Pt capillaries that were in turn sealed in 1.0-mm-diameter quartz capillaries. The loading was made

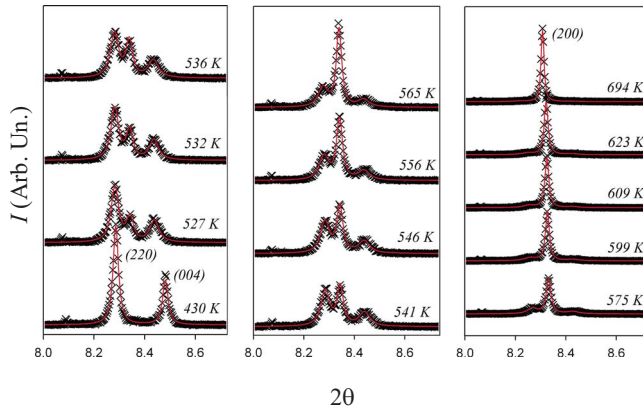


FIG. 1. (Color online) Details of selected XRPD patterns (count rate vs Bragg angle) as collected for different temperatures, referring to the $x=0.25$ composition sample. The crosses are the experimental points while the full lines are the results from the Rietveld refinement. The numbers in brackets are the Miller indexes of the diffraction peaks.

in a glove bag with N_2 inert atmosphere to minimize contact with oxygen and quartz.

Samples were investigated by x-ray powder diffraction (XRPD) using the high-resolution powder diffractometer of the beam-line ID31 at the ESRF, Grenoble, France.⁹ The wavelength of the incident x-ray beam ($\lambda=0.295130$ Å) was selected via a double-crystal Si(111) monochromator. Calibration and refinement were performed using a NIST standard Si powder ($a=5.43094$ Å).

During measurements the sample capillaries, which were mounted on the diffractometer axis, were spun and heated up to about 1173 K using a hot-air blower. Data were collected while warming at 2 K min^{-1} ($2 \leq 2\theta \leq 20^\circ$), and subsequently cooling at the same rate down to RT. For selected samples, isothermal data at suitable temperatures were also collected. Structural parameters and mass fractions were obtained by Rietveld refinement using the GSAS software suite¹⁰ and its graphical user interface EXPGUI.¹¹

III. RESULT AND DISCUSSION

Figure 1 shows the XRPD patterns at different temperatures for the $x=0.25$ sample, in a characteristic 2θ region. Below 500 K, only the peaks of the (2 2 0) and (0 0 4) reflections of the tetragonal structure are present. An impurity peak appears also, due to $K_2Mg_yCu_{1-y}F_4$, but in a very small amount (approximately 2% of the total sample weight) and thus the effect on the electronic properties of the system is negligible (see Ref. 6 for a full discussion on this point). Upon increasing the temperature the (2 0 0) reflection of the cubic structure appears. As it is evident from the relative peak intensities, the cubic phase amount increases with temperature while the amount of tetragonal phase decreases correspondingly. For $T \geq 673$ K the phase transition is almost complete. In addition, the full width at half maximum (FWHM) of the peaks is larger in the tetragonal phase than in the cubic one, meaning that the crystallite size is larger and/or strain is smaller in the cubic phase. The other samples

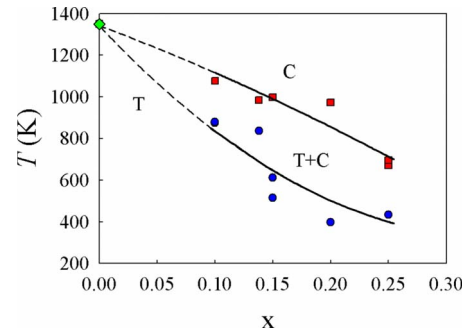


FIG. 2. (Color online) $KCu_{1-x}Mg_xF_3$ structural phase diagram in the Cu-rich zone. The existence fields of the cubic and tetragonal solid solution are drawn. Blue dots and red squares are experimental points derived from the analysis of the diffraction patterns for the different compositions: blue points refer to the appearance of the cubic phase, red squares to the vanishing of the tetragonal phase. The lines are guides to the eye drawn according to phase diagram topology. The extrapolation to $x=0$ is sketched by dashed lines; the green diamond is drawn accordingly. T and C stand for tetragonal and cubic phase, respectively.

behave in a similar manner, but the transition temperature increases as the Mg content is decreased, as shown below. The experimentally determined topology of the phase transition is typical of a first-order structural phase transition in a bicomponent phase diagram without miscibility gap: by increasing temperature a final monophasic state is reached starting from a different monophasic state through a biphasic one.

In Fig. 2 the phase diagram for $KCu_{1-x}Mg_xF_3$ is shown as obtained from the XRPD experimental data for the different compositions: measured transition temperatures are plotted versus Mg content, indicated as cation fraction (x). Experimental points are shown as blue dots and red squares, and the curves are guides to the eye drawn according to the topology of the structural phase diagrams; the curves are extrapolated to $x=0$ by dashed lines. The progression of the phase transition is shown in Fig. 3, in which the fraction of the cubic phase, playing the role of order parameter, is plotted versus T for the $x=0.25$ sample. To assess the nature of the phase transition, diffraction patterns have been collected at fixed temperatures as a function of time. The existence of an energy barrier for the transition is experimentally found in the time variation in cubic phase mass fraction, therefore demonstrating the phase transition to actually be of first-order type.⁶ As explained in detail in Ref. 6, the phase transition kinetics is diffusion limited. Double points for the same x in the plot refer to heating and cooling treatments, respectively. The presence of double points is due to the hysteresis of the heating-cooling cycle. The existence of hysteresis is clearly shown in Fig. 3, where the cubic phase mass fraction is plotted versus T , for the $x=0.25$ composition. It should also be noted that the point dispersion in Fig. 2 is due to the intrinsic difficulty in determining both the beginning (appearing of the cubic phase) and the end (disappearing of the tetragonal phase) of the phase transition by using the x-ray diffraction data. For the sake of better clarity, an illustrating example is given: blue dots and red squares in Fig. 3

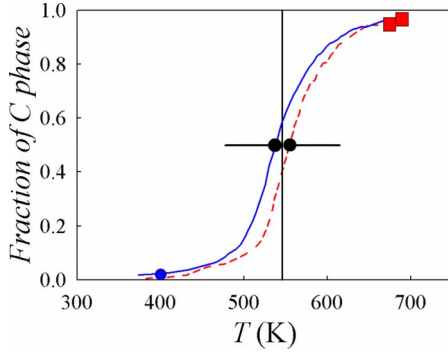


FIG. 3. (Color online) Order parameter, expressed as fraction of the cubic phase plotted vs T for the transition of the $\text{KCu}_{0.75}\text{Mg}_{0.25}\text{F}_3$ sample (red dashed curve: heating; blue solid curve: cooling). Blue dots and red squares in the inset mark the starting and end point of the phase transition for the $x=0.25$ composition sample, respectively. The black points are the inflection points of each sigmoid. The black vertical line marks the midpoint temperature used in Fig. 4 for the $x=0.25$ composition.

mark the starting and end points of the phase transition, respectively. The temperatures of these points have then been plotted in Fig. 2 for the $x=0.25$ composition sample as blue dots and red squares, accordingly.

However, the mid points of the phase transition (i.e., the temperatures at which the amounts of tetragonal and cubic phases are equal, or in other words, the inflection point in the sigmoids in Fig. 3) are much better determined (the error being around 1–2 K) and thus not affected by the above dispersion. Also in this case the procedure for determining these points is shown in Fig. 3. The inflection points of each sigmoid are marked as black points. The vertical black line marks the mean temperature of these points: this temperature has been considered as the midpoint of the phase transition.

Starting from these values, an estimate of the stabilization energy of the tetragonal (cJT-distorted) phase with respect to the cubic one can be derived. Since the phase transition is stated to be of the first order, the free energies of the two phases are the same when their amounts are equal.⁶ The internal energy difference between the two phases is therefore

$$\Delta U = kT \ln \alpha,$$

where α is the ratio between the degrees of freedom in tetragonal and cubic phase, and $\ln \alpha$ is a factor which is close to unit. Since $\ln \alpha$ is in any case constant and $\cong 1$ throughout different compositions in the $\text{KCu}_{1-x}\text{Mg}_x\text{F}_3$ system, kT gives a direct coarse estimate of the cJTd stabilization energy.

The energy derived in the above way is plotted versus Mg content x in Fig. 4. For each composition, the average of the various heating and cooling measurements is reported as one experimental point. The linearity of the cJTd energy behavior versus x is impressive, thereby enabling the extrapolation down to $x=0$ to be carried on trustworthily. For the undoped KCuF_3 the value of 0.116(5) eV [$T=1340(50)$ K] is readily found.

In the analogous system $\text{KCu}_{1-x}\text{Zn}_x\text{F}_3$, Tanaka *et al.*^{12,13} observed, employing the RXS technique, a rapid decrease upon increasing Zn concentration of both the scattering am-

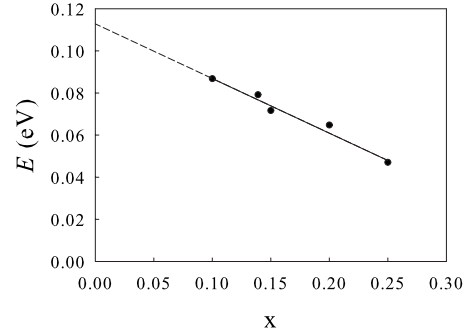


FIG. 4. Stabilization energy behavior of cJTd in $\text{KCu}_{1-x}\text{Mg}_x\text{F}_3$ as a function of Mg content. The data point distribution was fitted by a straight line ($r=0.988$, full line in the plot). By extrapolation to $x=0$, as indicated by the dashed line, a stabilization energy of 0.116(5) eV is obtained in the parent KCuF_3 .

plitude for the *forbidden* ($3/2\ 3/2\ 3/2$) reflection at the Cu K edge energy and a rapid reduction in T_{OO} (the temperature at which the forbidden reflection vanishes) versus x : they explained their findings in terms of dilution effects in the e_g orbital systems. We can now discuss these claims in the light of the present results. As mentioned above, the RXS signal in KCuF_3 is more sensitive to the distortion of the fluoride ions surrounding Cu rather than to the actual arrangement of the Cu $3d$ orbitals.⁵ Looking at the T_{OO} value for KCuF_3 as deduced from Ref. 12, one finds that the figure is close to 1200 K, a value not distant from what we obtained for cJTd. These two observations lead on one hand to the conclusion that the results presented in Refs. 12 and 13 should be (at least in the low x region) more directly related to the disappearance (or smearing out) of cJTd rather than being truthfully associated with OO. On the other hand, we have directly probed the structural degrees of freedom, as we used allowed reflections. Our results give therefore the correct interpretation of the driving force of the phase transition and a reliable estimate of the cJTd.

Actually, according to Pavarini *et al.*,³ Kugel-Khomskii superexchange mechanism in KCuF_3 gives rise to a phase transition with a fully ordered orbital state at $T_{\text{KK}} \cong 350$ K, a value that is remarkably large but not sufficient to explain the persistence of the distorted structure at high temperatures.³ In addition, the LDA+U calculations showed that the energy gain due to the distortion cannot be accounted for by the orbital polarization itself (Ref. 3 and references therein). The theoretical predictions in Ref. 3 are experimentally confirmed by the results reported in the present study: the persistence of the cJTd at T close to 1350 K is a clear indication that the electron-phonon coupling is the dominant mechanism stabilizing the KCuF_3 structure. In other words, our results experimentally demonstrate that the Coulomb repulsion just enhances the effects of lattice distortions¹⁴ rather than really driving the orbital polarization via superexchange,¹ opposite to conclusions drawn in previous publications on the subject.

IV. CONCLUSIONS

In conclusion, we have investigated the “melting” of the cJTd distortion in perovskite samples of composition

$\text{KCu}_{1-x}\text{Mg}_x\text{F}_3$, with x varying between 0.10 and 0.25. The transition relaxing the cJTd is found to be of first order and is detected at T increasing monotonically with x . From the transition temperature, an estimate of the cJTd stabilization energy is derived and found to increase linearly against x . The extrapolation to $x=0$ allows to disentangle the relevant energy scales of the pure KCuF_3 compound, and leads to a cJTd energy value of 0.116(5) eV. Our results strongly support recent LDA+DMFT calculations³ and indicate that the

electron-phonon coupling is the prevailing interaction in the stabilization process of KCuF_3 peculiar structure.

ACKNOWLEDGMENTS

The authors acknowledge the European Synchrotron Radiation Facility for provision of beamtime. Moreover, we would like to thank A. Rigamonti and S. Di Matteo for critical reading of this Brief Report and helpful discussions.

*Author to whom correspondence should be addressed. Dipartimento di Chimica Fisica “M. Rolla,” Università di Pavia, Viale Taramelli 16, I-27100, Pavia, Italy; paolo.ghigna@unipv.it

¹K. I. Kugel and D. I. Khomskii, *Sov. Phys. Usp.* **25**, 231 (1982).

²S. Kadota, I. Yamada, S. Yoneyama, and K. Hirakawa, *J. Phys. Soc. Jpn.* **23**, 751 (1967).

³E. Pavarini, E. Koch, and A. I. Lichtenstein, *Phys. Rev. Lett.* **101**, 266405 (2008).

⁴R. Caciuffo, L. Paolasini, A. Sollier, P. Ghigna, E. Pavarini, J. van den Brink, and M. Altarelli, *Phys. Rev. B* **65**, 174425 (2002).

⁵N. Binggeli and M. Altarelli, *Phys. Rev. B* **70**, 085117 (2004).

⁶M. Scavini, M. Brunelli, C. Ferrero, C. Mazzoli, and P. Ghigna,

Eur. Phys. J. **B65**, 187 (2008).

⁷C. Oliva, M. Scavini, S. Cappelli, C. Bottalo, C. Mazzoli, and P. Ghigna, *J. Phys. Chem. B* **111**, 5976 (2007).

⁸K. Hirakawa and Y. Kurogi, *Suppl. Prog. Theor. Phys* **46**, 147 (1970).

⁹A. N. Fitch, *J. Res. Natl. Inst. Stand. Technol.* **109**, 133 (2004).

¹⁰A. C. Larson and R. B. Von Dreele, Los Alamos National Laboratory Report LAUR No. 86-748 (2004).

¹¹B. H. Toby, *J. Appl. Crystallogr.* **34**, 210 (2001).

¹²T. Tanaka, M. Matsumoto, and S. Ishihara, *Phys. Rev. Lett.* **95**, 267204 (2005).

¹³T. Tanaka and S. Ishihara, *Phys. Rev. B* **79**, 035109 (2009).

¹⁴B. Halperin and R. Englman, *Phys. Rev. B* **3**, 1698 (1971).